Development of an Air-Conditioning Control System Responsive to Location and Intensity of Heat Source Using Thermal Sensors

Mr Long-ching Sin 冼朗正

BEng (Hons) in Architectural Engineering, City University of Hong Kong

Abstract: In this project, a ventilation control system that is responsive to the location and intensity of a heat source using a thermal sensor was designed. Making use of the sixteen sensing elements in an infrared sensor, a weighting that correlated with the distance between the sensing element and the fan was assigned to the temperature reading of each sensing element. The average weighted temperature was then used as the parameter to control the fan voltage. A control program was written in Arduino IDE to control the voltage of two fans. To facilitate the real-time monitoring of the heat source and the fan status, a processing program was written in Java to display the real-time data in colour boxes. The control model and the processing program were tested by a series of experiments using a lamp to simulate a heat source. Results proved that the average weighted temperature is a suitable parameter, and the proposed model satisfactorily controls the fans to operate at optimal voltage/speed in response to the temperature and location of the heat source in a fully automated and real-time manner. The system provides a user-friendly and economical design applicable to air-conditioning systems with a high potential of energy-saving. (200 words)

Keywords: Ventilation system, Control system, Thermal sensors, Arduino

Introduction:

Hong Kong, being a concrete jungle in the subtropical zone, relies heavily on the air-conditioning system to maintain thermal comfort and indoor air quality. All non-residential buildings in Hong Kong are serviced with air-conditioning. More than 80% of the local households have air-conditioners (EMSD, HKSAR, n.d.),. However, air-conditioning systems consume a high level of energy, took up 32% of the total electricity consumption in 2018 and stands out as the most significant in local electricity consumption (EMSD, HKSAR, 2020).

Although the technology of modern air-conditioning system has been invented for more than a hundred years (Wampler, 1949), scientists and engineers continue to seek improved designs of air-conditioners. In particular, air-conditioning control is one of the most popular research topics, which proves the pressing need for a balanced air-conditioning design that is user-friendly and energy-saving.

A Brief Review on the Modern Control Methods for Commercialised Air-Conditioners:

With the advancement in technology, a wider range of sensors such as thermal sensors, motion sensors etc. are available. While the concern of sustainability and energy-saving is growing globally, better methods to maintain thermal comfort at an optimal level are still exploring. Today, most of the top air-conditioner brands use a higher level of sensor technology to provide "smart" cooling in an energy-saving way. For illustration, six popular air-conditioning brands in Hong Kong are reviewed based on their online catalogues and official websites. Table 1 summarises the key sensor technologies used by them.

Table 1. Latest sensor technologies used by the top air-conditioner brands (Carrier, 2015; Mitsubishi Electric, 2020; Daikin Industries Ltd., n.d.; Fujitsu General, n.d.; Johnson Controls - Hitachi, n.d.; Panasonic, n.d.).

Features	**Daikin**	**Hitachi**	**Mitsubishi**	**Panasonic**	**Fujitsu General**	**Carrier**
1. Name of sensor tech	• Intelligent eye	• iSee and iSense	• 3D iSee	• ECONAVI	• Human sensor	• Follow Me
2. Nature of sensor	• Thermal	• Thermal and image	• Thermal	• Thermal	• Thermal	• Thermal
3. Sensor location	• AC unit	• AC unit	• AC unit	• AC unit	• AC unit	• Remote control handset
4. Operation of sensor	• Detects movement of	• iSense detects the occupancy	• Detects the outside	• Detects movement of	• Detects movement of	• Senses a location

	people and switches between normal operation and energy saving mode	and their location to step up/down airflow • iSense detects human activity and if detected at sleep, increases the temperature	temperature, the occupancy and their location and accordingly steps up/down the airflow	people and sunlight intensity and steps up/down the airflow accordingly	people and switches between normal operation and energy saving mode	temperature with the remote control and adjust the room temperature accordingly

Compared with the conventional design of air-conditioners, the most drastic advancement in recent years is the use of occupancy detection technology based on thermal and image sensing. Reviewing the top six brands of air-conditioners in Table 1, five out of six utilise thermal sensing technology (and image sensing as well in Hitachi) to detect human presence (Daikin Australia Pty Ltd., n.d.; Daikin Industries Ltd., n.d.; Fujitsu General, n.d.). If the room is detected unattended for a defined period, the unit will be switched to the energy-saving mode (+/- 2^{o}C in most brands). Mitsubishi and Panasonic are slightly more advanced to step up/down the airflow as well according to the number and location of occupants (Mitsubishi Electric, 2020, n.d.; Panasonic, n.d.). However, such adjustment in airflow is limited by a few discrete modes such as "high", "medium" or "low" only.

While the energy saving performance is promising in these commerialised air-conditioners, their control systems merely provide a standardised and stepwise adjustment of the temperature and airflow when the room is detected as unattended. The information captured by the thermal sensors is not fully utilised to achieve variable adjustment of the temperature or airflow in response to the location of the occupants inside the room. Furthermore, no spot cooling adjustment is made to increase the airflow when the skin temperature of the occupants increases. Since the accuracy and reliability of thermal sensors have been improved, more precise control system for air-conditioning installations can be explored to provide thermal comfort in a more energy-saving way.

Aim and Objectives:

The aim of this project is to design an economical control system for air-conditioning installation, which is responsive to the location and intensity of the heat source using thermal sensors. The objectives of this project include the following:

- To design a cooling control system that can respond to different heat locations using a thermal sensor.
- To design a cooling control system that can respond to different heat intensities using a thermal sensor.
- To investigate the energy-saving potential if using thermal sensors in control design.

Methodology:

Conceptual Model Design:

Based on the reviewed literature, a closed-loop control system was chosen to ensure the ventilating unit is responsive to temperature changes. The conceptual model of the control system is illustrated in Figure 1.

Due to the practicality concern, it is impossible to set up a vacant room with an air-conditioner and volunteers available to carry out the validation test. Therefore, an experimental setup that can be applied in the University laboratory condition was designed. This design also directly affected the control algorithm to be written.

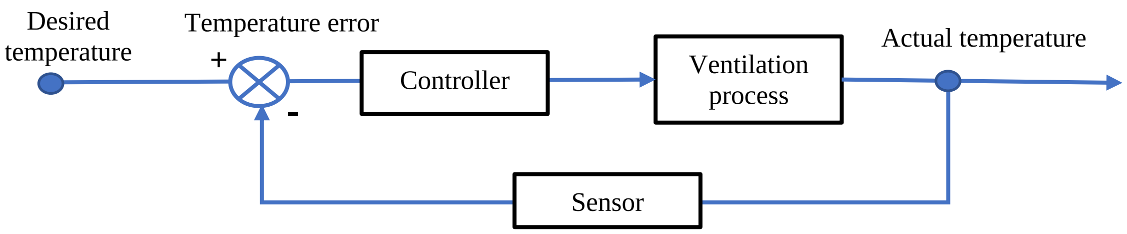

Figure 1. Conceptual model of the control system for this project.

Core Components of the Control Model:

Referring to Figure 1, the control system comprised with several core components. The screening and selection of the brand and model used for each component was made through an extensive search on the world wide web to fit the project setup and budget.

(1) Controller: Arduino UNO board Rev3, which is the latest version of Arduino Uno board, was chosen as the microcontroller. It is a highly popular controller for building automation control systems (Mahalakshmi and Vigneshwaran, 2017; Raju, Mahalingam and Rajendran, 2019; Widhiada *et al.*, 2019). It has 14 digital input/output pins and 6 analog inputs, operating in 5V and not more than 20V (Arduino, n.d.). It contains

everything needed in this project and can be connected directly to a computer with a USB cable. Furthermore, the web-based resource associated with Arduino provides a comprehensive toolkit for learning the program codes.

(2) Controlled element, i.e. the ventilating unit: 12V (0.15A) DC fans were used as these are the closest feasible alternative of an air-conditioner to be arranged in a laboratory. These fans can provide a high power with the fan speed adjustable by varying the voltage. Two DC fans were used in this project to allow cooling from two sides, the left-side and the right-side.

(3) Sensor: Omron MEMS thermopile sensor (D6T-44L-06) was selected to measure the temperature difference between the set point temperature and the heat source. Based on the literature review on the characteristics and technologies adopted in various thermal sensors, Microelectromechanical (MEMS)-based thermopile infrared thermal sensors is the ideal thermal sensor to be used in this project. These sensors can remotely detect the temperature of both stationary and moving humans, unlike infrared pyroelectric sensors that can only detect temperature changes in stationary objects (Omron Corporation, 2018).

Omron D6T-44L-06 was chosen due to its high popularity, accuracy and acceptable price. The D6T-44L-06 model has a total of sixteen sensing elements (4 x 4), giving a temperature reading for each field of view (FOV) from P0 to P15 (as shown in Figure 2). In other words, sixteen temperatures tagged with the respective sensing element can be recorded over the detectable area every time. Thes naming sequence of the sensing elements (P0 to P15) is fixed by Omron sensors for program codes and data record, and would be applied in the whole project. The power supply voltage required for the Omron sensor is 4.5 to 5.5V DC and it is sensitive at temperature ranges from 0 to 60°C (Omron, 2019). These operation characteristics fit our experimental setting and objectives.

(4) Heat source that can produce variable temperatures: a 200W incandescent lamp was adopted due to its low cost and zero hazard for use in a laboratory environment when compared with other alternatives such as hot plates or bunsen burners. While the simulation of human body temperature is in the range of 30 - 40°C, the 200W light bulb available in the laboratory is sufficient for the control model.

Other Miscellaneous Equipment for the Control Model:

Besides the core equipment mentioned above, other miscellaneous components are required for the control model or setting up of the tests. These include (1) a Motor driver L293D to provide the necessary current and voltage for the two fans, (2) a laptop for datalog and display of the real-time test readings, (3) a dimmer to control the light bulb temperature, (4) a switch mode power supply to convert AC to DC and to supply power to the fans, and (5) wires, solderless breadboard, clamps, stand and tripod for connecting the components.

Model Setup:

Based on Figure 1 and the components selected, the setup for the control system is shown in Figure 3.

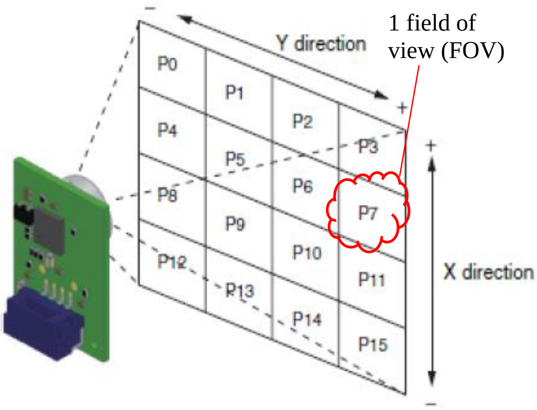

Figure 2. The 16 FOVs of OMRON MEMS D6T-44L-06 sensor (adapted from Omron Corporation, 2019)

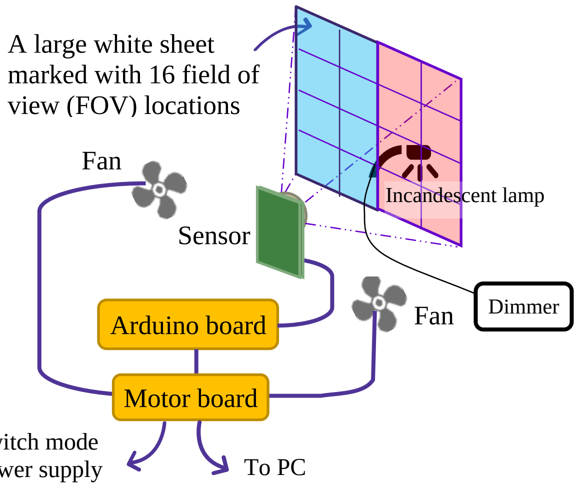

Figure 3. Diagrammatic illustration of the control model setup.

Control Program:

Before writing the program codes, the logic of the control system was drawn in the form of a flow chart (as shown in Figure 4). This flow chart can help the development, analysis and debugging of the program, which makes coding more efficient. Next, an open-source Arduino Software (IDE) version 1.8.13 was downloaded from https://www.arduino.cc/en/software for developing and testing the control algorithm. From the official website of Arduino, it supports both C and C++ languages. Therefore, C++ was used to write the program codes. Due to the limitation in the paper length, the control program codes are not elaborated here.

Trial Experiments to Establish the Model Parameters:

Before writing the program codes, some model parameters such as the weightings to temperature, the cycle time, the display on a laptop to monitor the experiments and the location of FOV centres must be identified. Many trials were done to establish these details for the best arrangement of the model design or the validation test setup. These parameters are briefly discussed below.

(1) Weightings to temperature

To control the fan speed in response to both temperature and location of a heat source, a weighting was applied to the temperature reading obtained at each sensor element with respect to its relative distance to the fan. The weightings were assigned according to Figure 5. Since two fans were used in this control model, the sensing area was divided into two halves, each half to be cooled by one fan. To allow finetuning of the weighting scale, a multiplier mechanism was applied to the weightings in the program. In the trial experiments, a multiplier of 1.2 was found to generate a desirable range of weighted temperatures for the fan voltage adjustment according to different heat source positions.

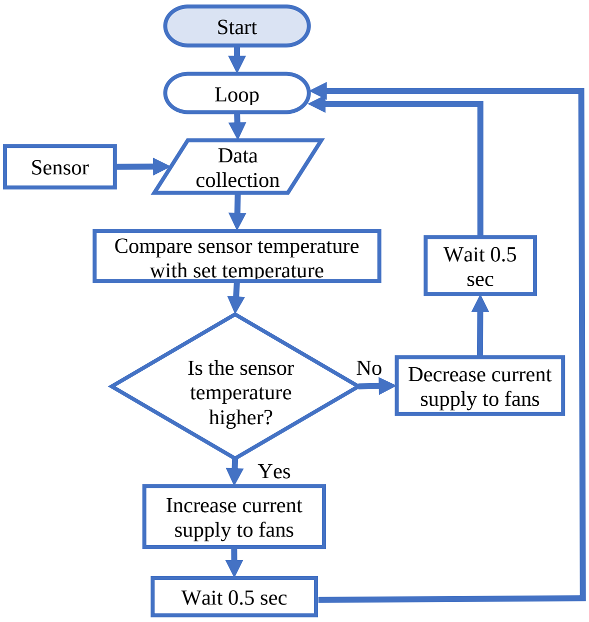

Figure 4. Flow chart of the proposed control system.

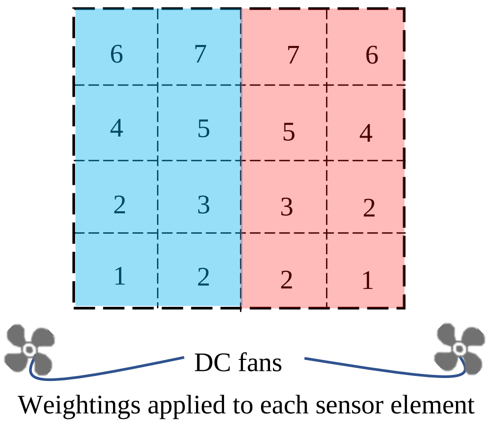

Figure 5. Weightings applied to 16 sensor elements.

(2) Cycle time

Cycle time refers to the duration set in the program to obtain a temperature reading from the sensor. According to the manufacturer's information, OMRON MEMS D6T-44L-06 sensors are capable to transmit a thousand data within a second. From the trials, it was observed that the cycle time of 0.5s was optimal to keep the control system sensitive enough to respond to the temperature changes.

(3) Display for sensor elements and fan speeds

In the trial runs, sixteen temperature readings were logged for every 0.5s on the laptop screen as shown in Figure 6a. Keeping track and interpreting the real-time status of the test, such as to check whether the temperature and position of the heat source was correct, was very stressful. To solve this problem, a processing program is necessary to process the real-time readings and display them on the screen in a colour box format that can be visualised and understand easily. Processing IDE 3.5.4 for macOS was used to process and display the sixteen sensor temperatures and two fan power percentages instantaneously. The Processing program was written in Java language. Moreover, the data was logged into a csv file for analysis and reporting purpose.

Before writing the processing program codes, some trial experiments were done to finetune the colour used and the temperature range so that the information can be visualised promptly. As shown in Figure 6b, dark red, bright red, pink and orange were used to represent temperatures range from very hot to cool. For the fans, dark blue, navy, light blue and black were chosen to represent fan voltage at high, medium, low and zero. The numerical figure in each colour box indicated the precise real-time reading. With the visual display, possible error such as wrong positioning of the heat source can be noticed immediately during the validation tests.

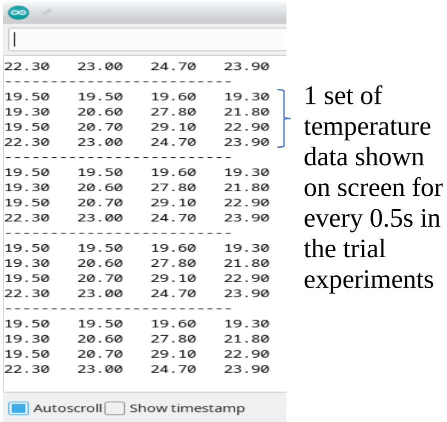

Figure 6a. Readings displayed without processing program

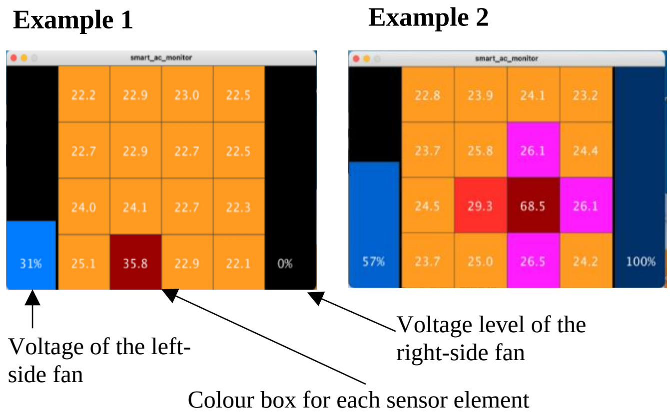

Figure 6b. Readings displayed with processing program.

Validation Tests Design for the Control Model:

A good control design process should include a final test to validate the performance of the system (Leigh, 2004). The setup of the validation test (in Figure 7), was basically the same as the control model in Figure 3.

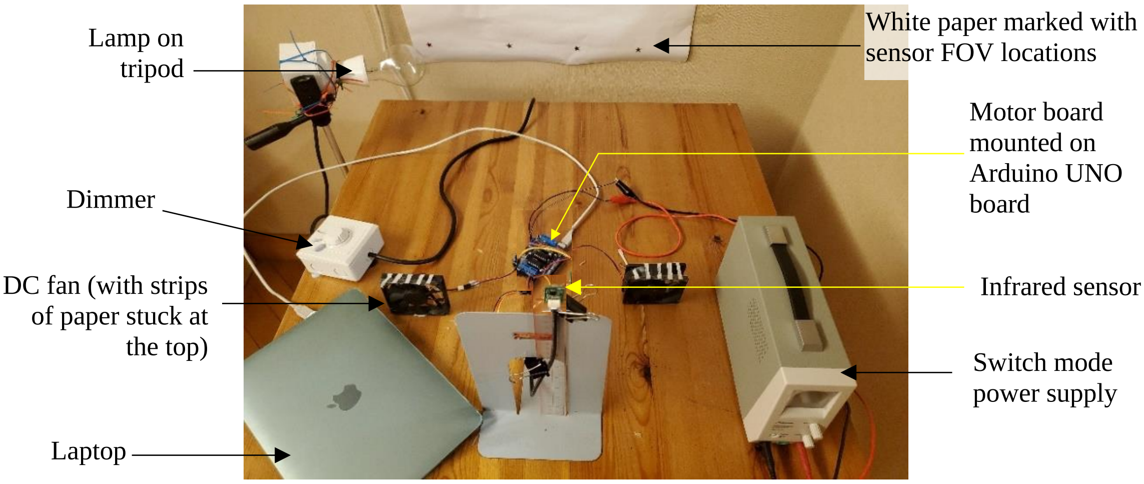

Figure 7. Experimental setup for the validation tests.

Two critical sets of validaiton tests were devised and reported here.

Set 1: The first test is to check whether the proposed control algorithm can adjust the fan speed in response to the temperature and location of a heat source. Setting at light bulb "low" (35°C), the fan voltage was recorded while moving the light bulb along the path as shown in Figure 8a over the white paper that had been marked with the centers of the FOV beforehand. The light bulb was held in each of these centers (hereinafter called "testing points") for around 5s to collect sufficient data. During the test, the laptop display was constantly monitored to ensure correct positioning of the light bulb. The test was then repeated with the lamp set at "medium" (65°C) and "high" (80°C) temperature levels.

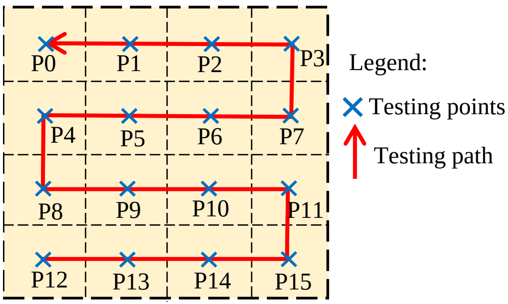

Figure 8a. Testing points and testing path in set 1 test.

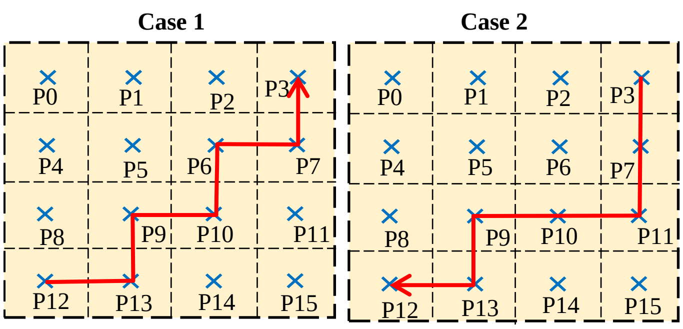

Figure 8b. Testing points and testing paths in set 2 tests.

Set 2: The second test was to simulate human movements within the detectable area. The light bulb at "low" temperature (35°C) was moved along the two paths as shown in Figure 8b. The fan voltages were recorded. The light bulb was held in each testing point for around 5s to ensure a sufficient amount of data was collected.

Results:

All the tests were completed smoothly in February 2021. The experimental setup was not altered during the test period. Throughout the validation tests, the processing program performed satisfactorily to display the colour boxes simultaneously with the lamp movement and in line with the temperature and fan voltage ranges. Figure 9 shows an example of a screen captured when the the lamp was placed at P13 under the "high" temperature level.

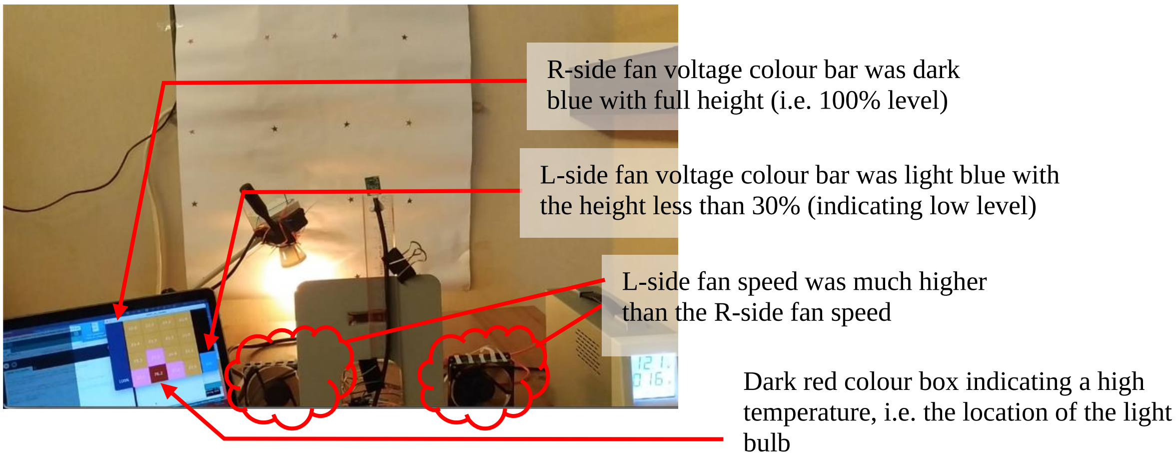

Figure 9. Screenshot of the validation test with the lamp set at the "high" temperature level placed at P13.

Due to the vast amount of readings recorded, only the average weighted temperatures were summarised here. Readings recorded when the light bulb was heating up or moving in between testing points were screened out to calculate the average. The average weighted temperature and fan voltages obtained in test 1 under "low", "medium" and "high" light bulb temperatures are tabulated in Table 2. Since the left-side fan was controlled by the weighted temperatures received from the eight sensing elements on the left, whereas the right-side fan was controlled by the temperatures from the other eight sensing elements on the right, a notation (L/R) was put adjacent to the testing points in Table 2 to highlight which side of the sensing area the light bulb was placed.

Table 2. Average weighted temperatures and fan voltage percentages at each testing point in test 1.

Testing points	Average weighted temperature (°C)						Fan voltage (%)					
	Low		Medium		High		Low		Medium		High	
	Left	Right	Left	Right	Left	Right	Left	Right	Left	Right	Left	Right
P0 (L)	31.4	27.2	37.10	28.06	39.79	28.16	100	0	100	15	100	18
P1 (L)	32.7	27.8	38.12	29.94	41.86	31.32	100	8	100	69	100	100
P2 (R)	27.7	32.9	29.32	42.32	30.70	44.20	5	100	51	100	91	100
P3 (R)	27.3	31.7	28.02	38.30	28.43	42.50	0	100	14	100	26	100
P4 (L)	31.1	27.2	35.58	27.96	40.42	28.18	100	0	100	12	100	18
P5 (L)	32.8	28.0	39.94	29.92	44.22	31.22	100	13	100	68	100	100
P6 (R)	28.2	32.5	29.49	40.08	30.67	44.33	19	100	56	100	90	100
P7 (R)	27.3	31.1	28.16	36.02	28.84	38.83	0	100	18	100	37	100
P8 (L)	29.6	27.4	32.57	28.05	34.42	28.12	60	0	100	15	100	17
P9 (L)	30.3	27.9	35.22	29.83	38.41	30.16	80	10	100	66	100	75
P10 (R)	28.0	30.0	29.42	34.93	30.77	37.52	13	72	54	100	93	100
P11 (R)	27.3	29.2	28.14	32.39	28.63	34.95	0	47	17	100	31	100
P12 (L)	27.9	27.0	29.18	27.36	30.09	27.72	9	0	47	0	73	5
P13 (L)	28.9	27.2	31.74	28.06	33.02	28.56	40	0	100	15	100	29
P14 (R)	27.4	28.7	28.42	30.89	28.96	32.89	0	34	26	96	41	100
P15 (R)	27.3	28.0	37.10	28.06	28.25	30.96	0	14	100	15	21	98

Similarly, the fan voltages and the average weighted temperatures recorded for case 1 and case 2 simulations in test 2 were listed in Table 3.

Table 3. Average weighted temperatures and fan voltage percentages at each testing point in test 2.

Case 1					**Case 2**				
Testing points	Average weighted temperature (°C)		Fan voltage (%)		Testing points	Average weighted temperature (°C)		Fan voltage (%)	
	Left	Right	Left	Right		Left	Right	Left	Right
P12 (L)	27.68	26.76	5	0	P3 (R)	27.07	29.89	0	68
P13 (L)	28.39	26.92	25	0	P7 (R)	27.30	29.68	0	61
P9 (L)	29.73	27.23	63	0	P11 (R)	27.19	28.42	0	26
P10 (R)	27.69	29.45	5	55	P10 (R)	27.73	29.14	6	46
P6 (R)	28.02	31.03	14	100	P9 (L)	29.31	27.37	51	0
P7 (R)	27.41	30.21	0	76	P13 (L)	28.52	27.02	28	0
P3 (R)	27.33	30.14	0	75	P12 (L)	27.61	26.88	2	0

Data Analysis and Findings:

Responsiveness to the Heat Source Location and Intensity:

From the "low" temperature level results of test 1 (Table 2), the fan was turned on to a relatively higher voltage when the light bulb was placed farther away from its side. The other fan was not turned on or at a very low voltage level to save energy. The overall fan voltages were higher when the lamp temperature was set at "medium" level and the highest at the "high" level. Furthermore, under the "high" temperature level, six testing points (P1, P2, P5, P6, P9 and P10) had one fan fully operated and the other fan operated at 75% capacity or more. All these testing points were lain at the center of the sensing area, which were the most distant from the two fans. Since the light bulb temperature at the "high" level was around 80°C, greater power from both fans was activated. Such a result was not observed in the "low" or "medium" temperature tests. The findings evidenced that the fan voltage was successfully controlled in accordance with the temperature of and the distance from the heat source.

To demonstrate the responsiveness of the control model better, the relationship between the light bulb temperature level and its position against the fan voltage was plotted in Figure 10a to Figure 10d. Since the left fan results exhibited a similar pattern as those of the right fan, only the voltage graphs for the right fan are shown here to save space. For clarity, the fan voltage output data were divided into four groups according to the horizontal distance of the testing points to the right-side fan, with each group illustrated by a separate graph.

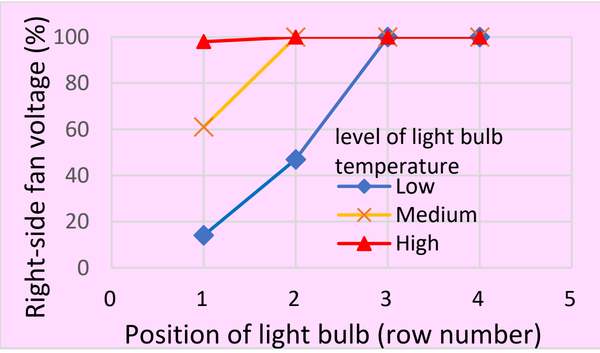

Figure 10a. Testing at P15, P11, P7 and P3 with three levels of heat source temperature

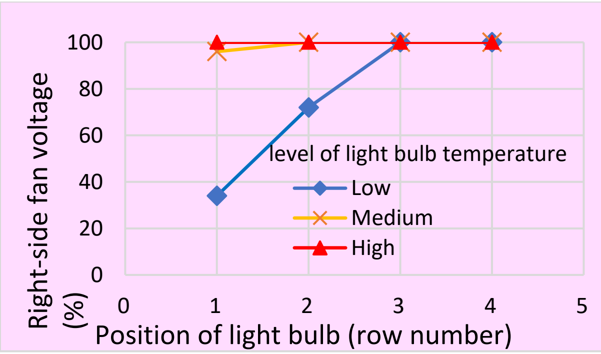

Figure 10b. Testing at P14, P10, P6 and P2 with three levels of heat source temperature

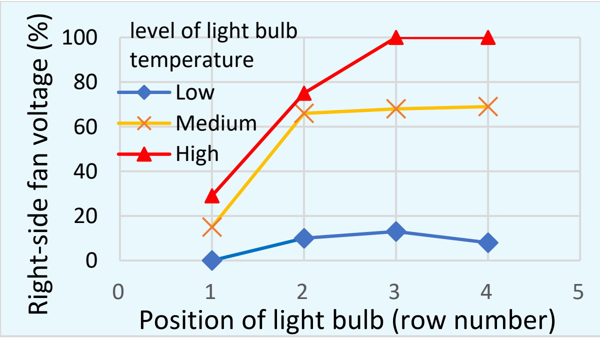

Figure 10c. Testing at P13, P9, P5 and P1 with three levels of heat source temperature

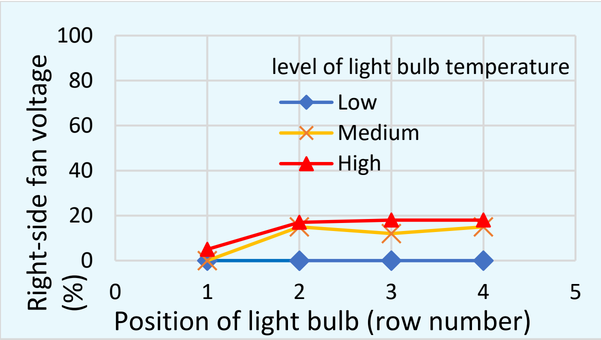

Figure 10d. Testing at P12, P8, P4 and P0 with three levels of heat source temperature

All the graphs in Figures 10a to 10d show that the higher temperature of the heat source (light bulb), the greater voltage output of the fan. The red curve that represents "high" light bulb temperature is always at the top whereas the blue curve that represents "low" light bulb temperature is at the bottom. Regarding the responsiveness to the location of heat source, an increase in the fan voltage was observed when the light bulb was farther away from the fan. This can be identified from two directions. First, the curves exhibited an upward trend, reflecting that the fan voltage increases as the light bulb moves vertically from the bottom to the top of the sensing area. Second, the right-side fan was designed to respond to the heat source/gain on the right-half of the sensing area. Therefore, its responsiveness (as reflected by the fan voltage) was the lowest when the light bulb was placed at P12, P8, P4 and P0 (Figure 10d), but slightly higher in the central axis along P13, P9, P5 and P1 (Figure 10c) due to the possible heat transfer to the adjacent axis with high weightings (P14, P10, P6 and P2). The voltage output was the highest at P14, P10, P6 and P2 (Figure 10b) as the right-side fan was farther away from these points when compared with P15, P11, P7 and P3 (Figure 10a). These results indicate that the fan voltages were adjusted according to the horizontal distance from the heat source.

Simultaneous and Variable Response to the Change in Location and Intensity of Heat Source:

The effectiveness of the control model to provide simultaneous and variable response was best demonstrated in the set 2 test. Graphs were plotted between the fan voltages and the number of moves. Figure 11 and Figure 12 illustrate the fan voltage profile when the simulated human (light bulb) moved along the case 1 path and case 2 path respectively. It is obvious that the fan voltages increased when the simulated human moved farther away from the fans (e.g. from step 4 to step 5 in case 1) and vice versa (e.g. from step 6 to step 7 in case 2). More importantly, the voltage was variable in the full range from 0 to 100% (instead of stepwise) according to different temperature levels and/or heat source locations.

During the tests, it is observable from the labtop real-time colour display that the voltage of the two fans changed simultaneously with the movement of the light bulb.

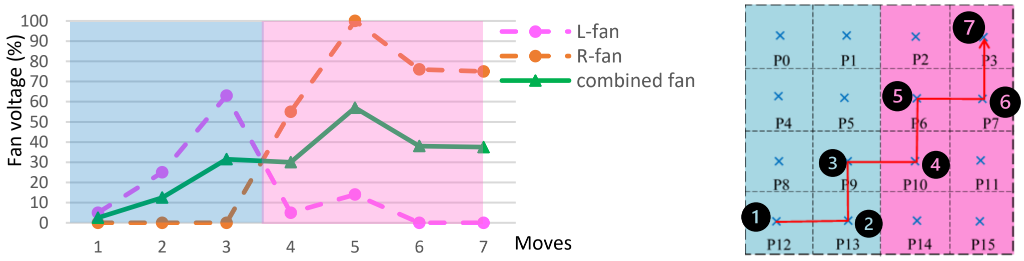

Figure 11. Fan voltage output with light bulb simulating human movement in case 1.

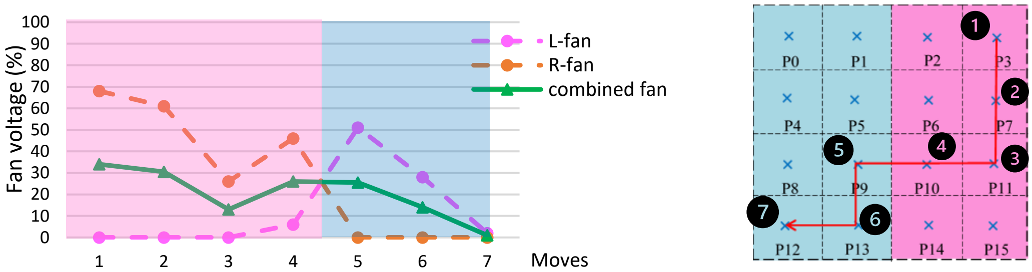

Figure 12. Fan voltage output with light bulb simulating human movement in case 2.

Energy Saving Potential:

With one fan assigning to regulate one half of the sensing area, validation results indicated that the two fans operated in a complementary manner. For example, in Figure 11, when the lamp moved from step 3 to step 4 (from the left half to the right half of the sensing area), the right fan voltage climbed whereas the left fan voltage dropped. This allows more localised cooling to improve thermal comfort while saving energy. Similar situation can also be found in case 2 (Figure 12) when moving the lamp from step 4 to step 5. In reality there are frequent movements of the occupants within an air-conditioned area. Without sacrificing thermal comfort, the potential of energy saving remains high if adopts the proposed control system in the air-conditioning design.

Discussions:

Firstly, the three objectives of this project were achieved satisfactorily. From the data analysis, it is evidenced that the proposed model can successfully control the fan speed in response to the heat source temperature and its location. Energy saving potential is promising if applied the control model in an air-conditioning system. Results indicated that the fans can be operated in a complementary manner to reduce the overall energy consumption while providing targeted cooling.

Secondly, it is confirmed that the average weighted temperature is a good parameter to represent the temperature and the location factors in the control algorithm. The multiplier successfully stretched the weighted temperatures to a suitable range for effective control. The use of multiplier can flexibly finetune the weightings when the room temperature varies. Thirdly, the set 2 validation test results reveal that the thermal sensors can perform motion tracking successfully. The fan voltage was adjusted simultaneously with the light bulb movement due to the short cycle time of data reading. If both the sensing area and the number of sensing elements are increased (such as using the highest grade Omron sensor with 16 x 16 sensing elements (Omron Electronic Components BV, 2013)), changes in the occupant position or even body posture can be detected in a finer measurement grid. In this way, additional features such as ventilation control responsive to human movement/activities e.g. sitting, doing fitness exercise, sleeping etc. will be possible.

Finally, the processing program written to display the real-time status of the measurements and control parameters is crucial and helpful. Strictly speaking, the control program can be operated without the processing program. However, with the processing program, adjustment to the light bulb position can be made duly when the targeted colour box is not indicating the highest temperature colour. The voltage bars also help to indicate whether the fan is operating properly. The visual display of these colour boxes/bars is definitely easier to interprete, allowing prompt corrections to be made during the tests. It is understandable why a good control system often designs with a visual monitoring system that provides colourful real-time display of the equipment/control status.

Potential Benefits of This Study:

From the validation test results, several potential benefits of the proposed system can be identified. First, with the use of the control program in the ventilation system, the two fans are operated in a complementary way. The fan speed can be optimised with respect to the distance between fan and the heat source. Spot cooling or localised cooling can be delivered under the proposed system as well. This saves the energy consumption while maintaining a desired level of ventilation. Second, since the thermal sensor is highly responsive (in the current design the cycle time is 0.5s), changes in the sensing area temperature can be detected instantaneously to vary the fan speed. This performance is recognised in the set 2 validation test when simulating a human moving in the sensing area randomly. The fan voltage was adjusted simultaneously with the heat source movement. Third, with the control program, the fan speed can be automatically adjusted according to the movement of the heat source in a real-time manner. No manual adjustment is required. This feature is especially useful when the occupants are not free to adjust the ventilation speed, e.g. when they are doing fitness exercise. Fourth, a better level of thermal comfort can be achieved as the intensity and the source of ventilation will be adjusted according to the heat source temperature and location, rather than being fixed at a constant level at all times. Fifth, the colour box display processing program designed with the control system provides a visual monitoring tool. Operators and maintenance staff can visualise the fan voltage as well as the heat source location and intensity effectively from the computer screen in a real-time manner. Therefore, care should be taken when screening and analysing the data.

Limitations:

Although calibration of the infrared sensors is often suggested (Chen and Chen, 2016), no calibration of the infrared sensor was conducted due to the lack of equipment. Considering the primary objective of this project is to develop a control model for the ventilation system, the possible discrepancy between the true temperature and the sensor reading can be absorbed by the weighted temperature. In addition, a light bulb was used to simulate a human body in the validation tests. This enables a smaller-scaled test to be done in the laboratory. However, the light bulb is relatively small, which results in a higher variation in the temperature readings as it may not be placed at the centre of the FOV. Also, the spread of radiant heat from the light bulb is significant. These factors increase the fluctuation of the temperature readings during the tests.

Future work:

With the wide range of sensors available in the market, other sensing technologies can be applied in air-conditioning control. For example, air quality is a prevalent concern in modern HVAC designs. Control models can be developed to monitor and adjust the ventilation rate by using CO_2 sensors to detect the level of CO_2. Also, the reliability of using thermal sensors for motion sensing and tracking can be further explored to enhance the ventilation system features such as automatic on/off control based on occupancy level.

Conclusions:

In this project, an infrared sensor was used to control a ventilation system so as to respond to different locations and intensities of a heat source. Using two DC fans as the ventilation system and a light bulb to simulate the heat source, the performance of the proposed control system was validated by a series of experiments. Results evidenced that the DC fan voltages (so as the fan speeds) increased when the light bulb temperature was higher or when the light bulb was farther away and vice versa. The control model was proven as successful with all the planned objectives achieved. The processing program written for monitoring the real-time status of the control system was also effective. The proposed control model presents a feasible energy-saving solution which can provide variable cooling in response to the heat source intensity and location in an automatic and instantaneous manner. Finally, this project affirms the strengths of thermal sensors, which can be further exploited in commericalised ventilation systems.

References:

Arduino (n.d.) ‘Arduino Uno Datasheets’. Available at: https://www.farnell.com/datasheets/1682209.pdf (Accessed: 23 December 2020).

Carrier, U. T. (2015) *Carrier - Remote Controller Owner’s Manual*. Available at: https://en.ahi-carrier.gr/wp-content/uploads/sites/2/2017/06/Remote-Controller-Manual-QHM_EN.pdf (Accessed: 30 December 2020).

Chen, H. Y. and Chen, C. (2016) ‘Determining the emissivity and temperature of building materials by infrared thermometer’, *Construction and Building Materials*, 126(15), pp. 130–137.

Daikin Australia Pty Ltd. (n.d.) ‘Daikin Split System Air Conditioners’. Available at: https://climateheatcoolservices.co.nz/FINAL_Split_Brochure.pdf (Accessed: 20 December 2020).

Daikin Industries Ltd. (n.d.) ‘Daikin Room Air Conditioner Operation Manual (Inverter)’. Available at: https://www.daikin.com.au/sites/default/files/daikin-split-system-L-Series-FTX%28K%29S20-95LVMA.pdf (Accessed: 20 December 2020).

EMSD, HKSAR (2020) ‘Hong Kong Energy End-use Data 2020’. Available at: https://www.emsd.gov.hk/filemanager/en/content_762/HKEEUD2020.pdf.

EMSD, HKSAR (n.d.) ‘Residential Air Conditioning: An Energy Efficient Guide’. Available at: https://www.emsd.gov.hk/filemanager/en/content_718/EMS_Energy(low-res).pdf.

Fujitsu General (n.d.) *Core Technology*. Available at: https://www.fujitsu-general.com/global/products/split/technology/index.html (Accessed: 30 December 2020).

Johnson Controls - Hitachi, A. C. I. Ltd. (n.d.) ‘Every Home Deserves a Hitachi Inverter AC’. Available at: https://www.jci-hitachi.in/images/products/specifications/iConnect-catalogue_1523963684.pdf (Accessed: 25 December 2020).

Leigh, J. R. (2004) *IEEE Control Engineering Series 64 - Control Theory, 2nd Edition*. Edited by D. Atherton, G. W. Irwin, and S. Spurgeon. London, U.K.: The Institution of Electrical Engineers.

Mahalakshmi, G. and Vigneshwaran, M. (2017) ‘IOT based home automation using arduino’, *International Journal of Engineering and Advanced Research Technology*, 3(8), pp. 7–11.

Mitsubishi Electric (2020) *‘Sensing’ Your Needs: The Key to Personalized Comfort*. Available at: https://www.mitsubishielectric.com/en/our-stories/article/xx_ww_s_in2006_01.page (Accessed: 30 December 2020).

Mitsubishi Electric (n.d.) *3D i-See Sensor Technology*. Available at: https://www.mitsubishi-electric.co.nz/heatpump/3D-i-See-Sensor.aspx (Accessed: 30 December 2020).

Omron (2019) ‘MEMS thermal sensor D6T catalogue’. Omron.

Omron Corporation (2018) ‘MEMS Thermal Sensors D6T (Cat. No. A274-E1-04)’.

Omron Corporation (2019) ‘MEMS Thermal Sensor D6T - User’s Manual’. Omron.

Omron Electronic Components BV (2013) ‘Infrared MEMS Thermal Sensor’.

Panasonic (n.d.) *ECONAVI Technology*. Available at: http://www.panasonic.hk/english/tech/econavi_air_conditioner.aspx (Accessed: 30 December 2020).

Raju, P. S., Mahalingam, M. and Rajendran, R. A. (2019) ‘Design, implementation and power analysis of pervasive adaptive resourceful smart lighting and alerting devices in developing countries supporting incandescent and led light bulbs’, *Sensors*, 19, p. 2032.

Wampler, C. (1949) *Dr. Willis H. Carrier: Father of Air Conditioning*. Newcomen Society of England, American Branch.

Widhiada, W. *et al.* (2019) ‘Temperature stability and humidity on infant incubator based on fuzzy logic control’, in. *5th International Conference on Computing and Artificial Intelligence*, Bali, Indonesia.